

# Characterization of slow faulting with subdaily GPS positioning

Webb, F H

[fhw@jpl.nasa.gov](mailto:fhw@jpl.nasa.gov)

Jet Propulsion Laboratory, M/S 238-600 4800 Oak Grove Dr, Pasadena, CA 91109 United States

Melbourne, T I

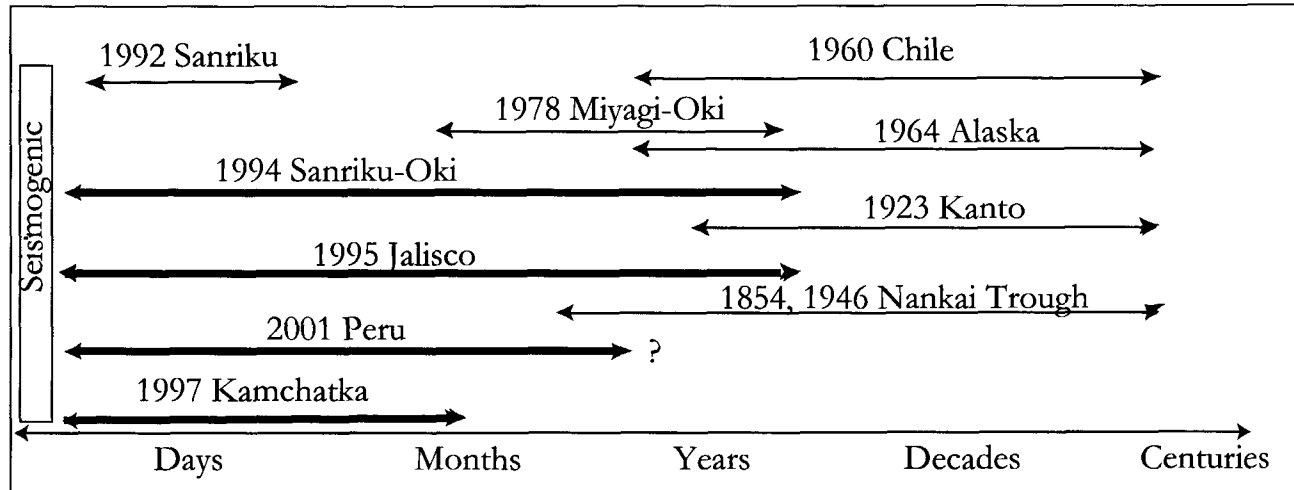
[tim@geophysics.cwu.edu](mailto:tim@geophysics.cwu.edu)

Central Washington University, Dept. of Geological Sciences 400 E 8th Ave., Ellensburg, WA 98926 United States

Over the last several years, data from continuously operating GPS stations have been used to detect transient deformation associated with large subduction zone earthquakes. Recently, the  $M_w=8.4$  June 23, 2001 Peru earthquake ruptured the Nazca-South American plate interface to become the largest event in the last 30 years. The mainshock was followed by a vigorous aftershock sequence, including three events with moment magnitudes of  $M_w=6.7$ ,  $6.5$ , and on July 7, an  $M_w=7.6$  event. Two-hour position estimates from a continuous GPS station located at Arequipa, Peru, document transient deformation at time scales from hours to days. These signals are obscured by daily position estimates highlighting the need for utilizing sub-daily positioning to increase our ability to detect transient aseismic faulting.

Station positions are estimated as stochastic processes with white noise resets every 2 hours using 24-hour data arcs. By applying stochastic resets to the coordinates only, the geometric strength of the 24-hour data arc for estimating carrier phase biases and atmospheric delays is retained. Station position estimates are thus obtained at a higher rate without significant systematic artifacts associated with higher frequency error sources. While modeling station positions as a white noise process may produce a time series that is noisier than a random walk model, it is a more conservative approach to identifying transient deformation. With this estimation scheme, subsequent position estimates remain uncorrelated in time, which is not the case with random walks. Moreover, the white-noise approach side-steps the need to establish an a priori rate of random walk process noise which neither suppresses a true signal nor introduces erroneous deformation artifacts.

### Time scales of observed postseismic transients



*After Melbourne et al., 2002*

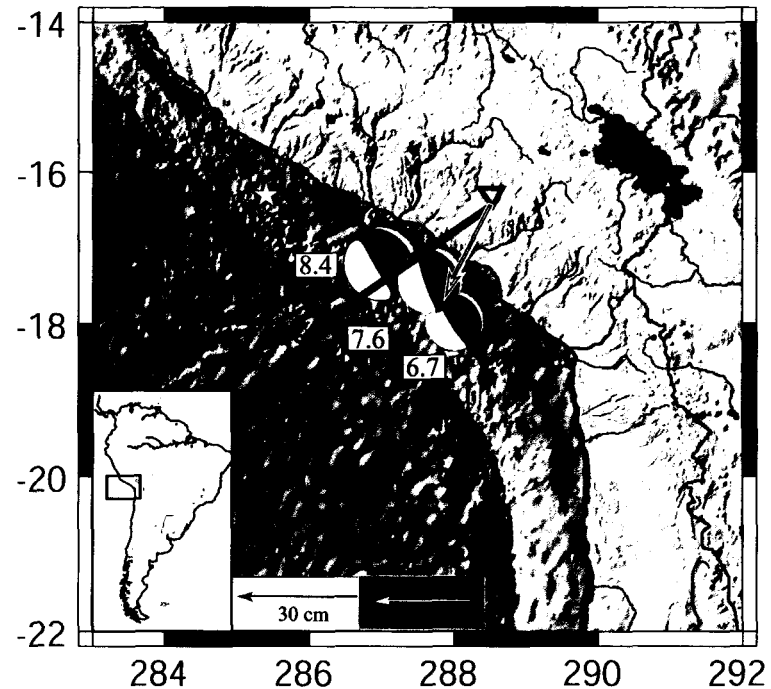
Observed spectrum of postseismic moment release following great subduction earthquakes.

Older events, measured with campaign triangulation or leveling, show deformation over months to years.

More recent events, captured with continuous GPS, show that it is not unusual for deformation to occur over timescales starting at the seismogenic and extending through hours, days, and weeks

The continuously operating GPS station operated by NASA for the International GPS Service (IGS) located at Arequipa (AREQ), Peru, recorded both coseismic and post-seismic signals from the earthquake.

While the data from most GPS stations is processed in daily batches for daily station positions, following large earthquakes, subdaily processing of the GPS data allows significant postseismic signals to be detected.



Measured GPS offsets during the 06/23/01  $M_w = 8.4$  Peru mainshock and aftershocks. Solid black vector shows coseismic displacements due to the mainshock, white vector denotes measured preseismic offset prior to the July 7  $M_w = 7.6$  aftershock. Error ellipses are 2s. White star shows National Earthquake Information Center rupture nucleation site. Triangle denotes position of the IGS GPS station located at Arequipa, Peru.

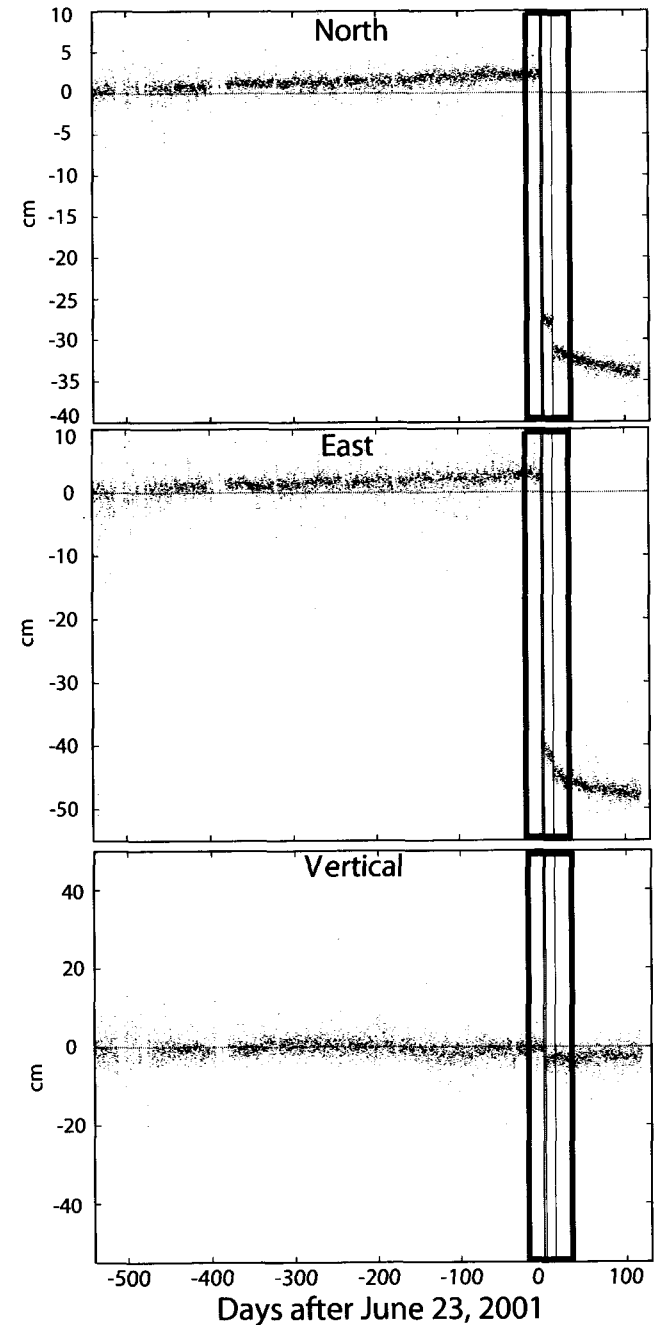
Several authors have reported and described techniques for subdaily analysis (e. g., Bock, et al., 2000. Larson, et al. 2001, Elosegui, et al., 1996, Webb, 1992).

In this poster we describe the results and techniques from the analysis of data from the IGS station AREQ.

The analyses were performed using the GIPSY software, precise point positioning, and whitenoise resets on the station positions every two hours. Satellite parameters (orbits and clocks) were fixed to JPL's submission to the IGS. Oceanloading coefficients are from the model of Scherneck, (1991) using the GOT00 tidal model. Zenith tropospheric delays were estimated along with tropospheric gradients.

These results reveal the co-, post-, and a pre-seismic displacements of the station in a global reference frame.

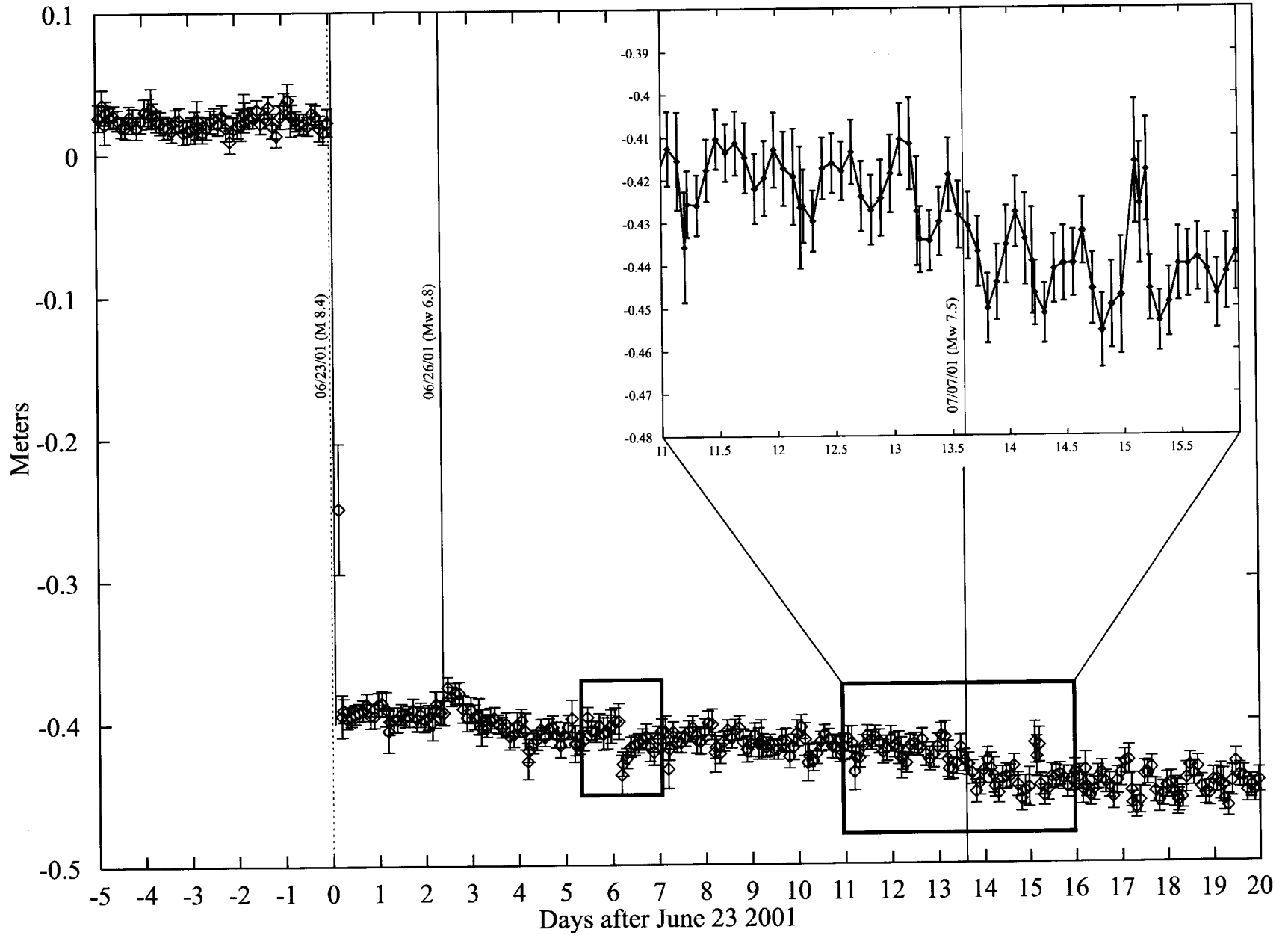
Two hour position solutions show interseismic, coseismic and postseismic deformation recorded at Arequipa between two years prior to and 9 months after the June 23 2001 Mw = 8.4 event. Heavy black squares denote zoom area shown in following figures. Thin solid black lines show times of seismogenic rupture reported by the Global Seismic Network.  $\chi^2$ -fit of interseismic strain accumulation rates in the north, east and vertical components measure  $1.2 \pm .02$ ,  $1.6 \pm .02$ , and  $0.26 \pm .04$  cm/year, respectively.

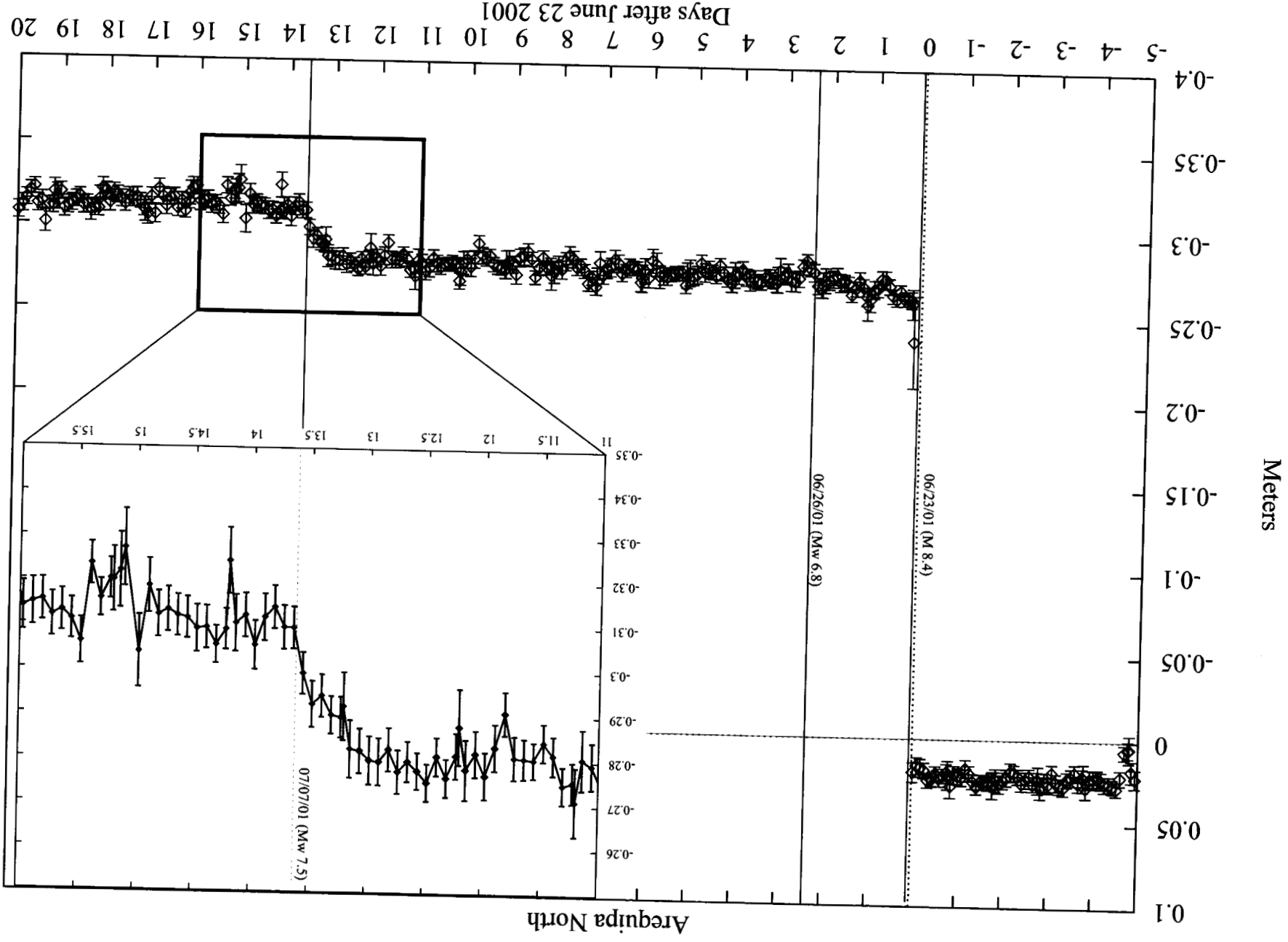


The adjacent figures show the 2-hour solutions for the coseismic deformation recorded at AREQ from the mainshock and two major aftershocks. Vertical lines denote times of major aftershocks. Preseismic deformation prior to the July 7 Mw = 7.6 aftershock is visible on the north and east components.

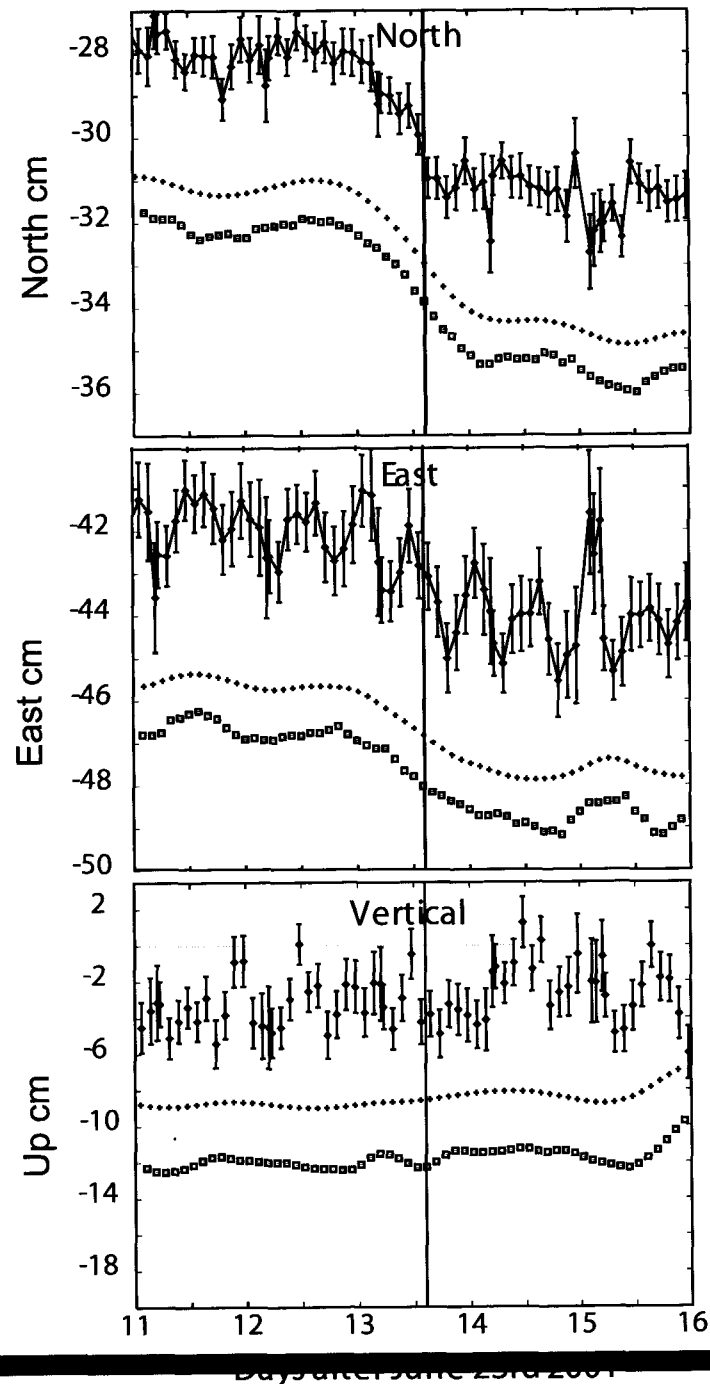
The zoom of the five-day period around the July 7 aftershock (inset and last panel) shows that on the north component, where signal scatter is lowest and preseismic deformation signal is largest, deformation starts 18 hours prior to the aftershock. On the east component, the significant <3 cm offset on June 29th, six days after the mainshock, shown inside the dashed box, does not correspond to any teleseismically reported earthquake. Its total duration is less than 6 hours, during which time the position returns to the mean value for the two days prior to and after the jump.

# Arequipa East





The figure at right shows a clear pre-seismic signal prior to the largest aftershock. The signal is 3-sigma greater than the noise on the preceding 5 days of 2-hour positions. In addition, no rate change of this magnitude is present in the more than 7000 18-hour periods in the time series prior to the June 23 earthquake. This anomaly only occurs in the station coordinates. Receiver SNR, and receiver clock, tropospheric delay and gradient estimates show no unusual behavior during this period.



Crosses are computed with an acausal  $n = 3$  symmetric smoothing window, squares a causal, single-pass Butterworth filter with a 12-hour corner. Both filtered time series show 2 cm of southerly and 1 cm of westerly preseismic motion. No deformation is visible on the vertical component.

In most cases, the noise on the subdaily positions is controlled by the data strength and geometry for determining the carrier phase biases as real values and by the level of signal multipath.

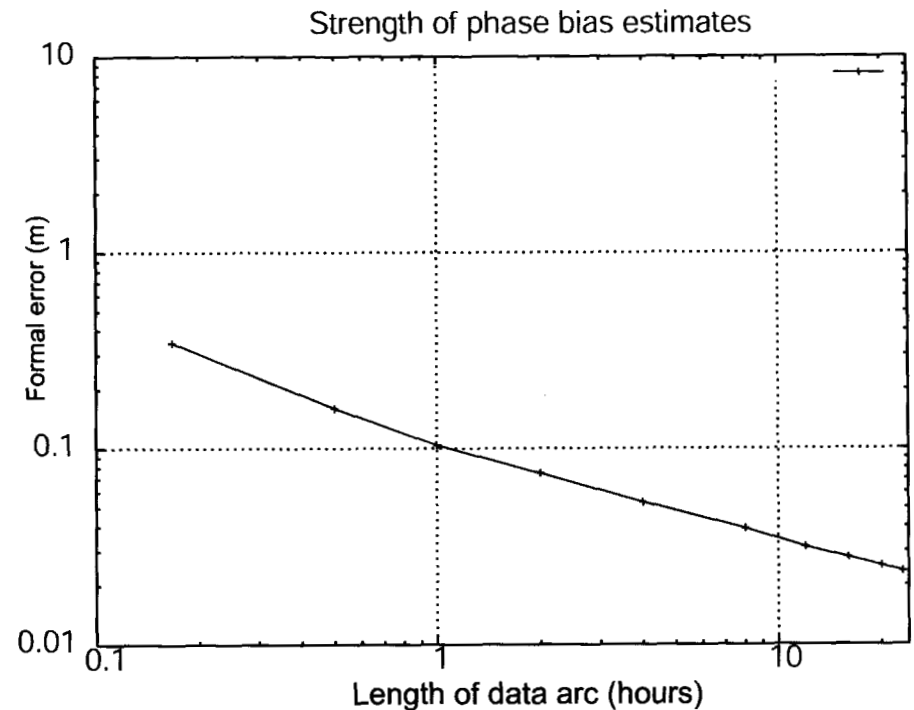
The figure at right shows the formal error for estimates of the phase biases for different data arc lengths and shows that for short data arcs, the parameters are only weakly determined.

Additional improvement can be obtained if the biases, within the context of a network solution, can be resolved/fixed to their double differenced values.

With the appropriate estimation strategy the phase bias parameters can be well enough determined that carrier phase multipath would be the dominant noise source.

Multipath noise can cause several centimeters of position error and is site dependent. Techniques for removing it have been successfully demonstrated to provide high precision results (Bock, et al., 2000). The technique uses data from the previous 3 days to estimate the site multipath and remove it from the current day of interest.

During a period of potential seismic transients, it may be difficult to apply this technique and separate transients and aftershocks from multipath.



The technique of whitenoise resets on the station positions has been applied to the analysis of more than 10,000 km of kinematic GPS surveys in support of SRTM (Webb, et al., 1999). In these cases, whitenoise resets were performed at every epoch and resulted in 2, 2, and 10 cm of position error in the north, east, and vertical components of position.

This represents a limit on this technique due to multipath in the area of the antenna when the reset interval is equivalent to the sampling interval.

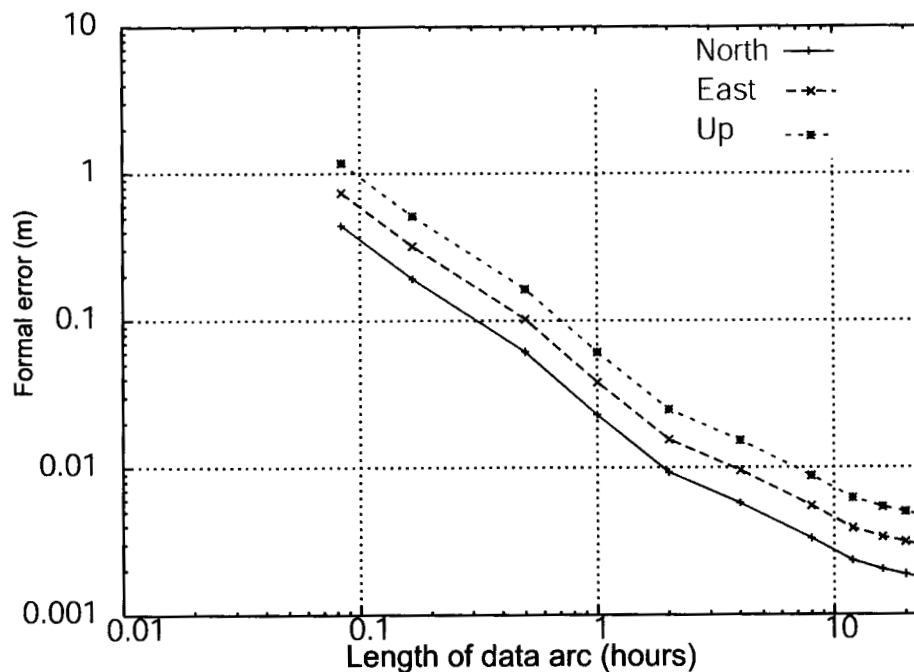
In the results here, we attempt to mitigate the effects of multipath by using a whitenoise reset interval of 2 hours.

An alternative approach to whitenoise resets would be to apply a correlated model, such as a random walk model. *Larson, et al.*, 2001 have discussed this model in detail as it applies to volcanic processes. The application of this model requires that an a priori rate be established for adding the process noise which neither suppresses a true signal nor introduces erroneous deformation artifacts. Since there could be discrete displacement events during the aftershock sequence, the determination of the best rate may be impractical and could over constrain the solution.

An alternative to whitenoise resets is to cut a 24 hour RINEX file into n-files that are x-hours long, and then process each file separately to obtain sub-daily positions.

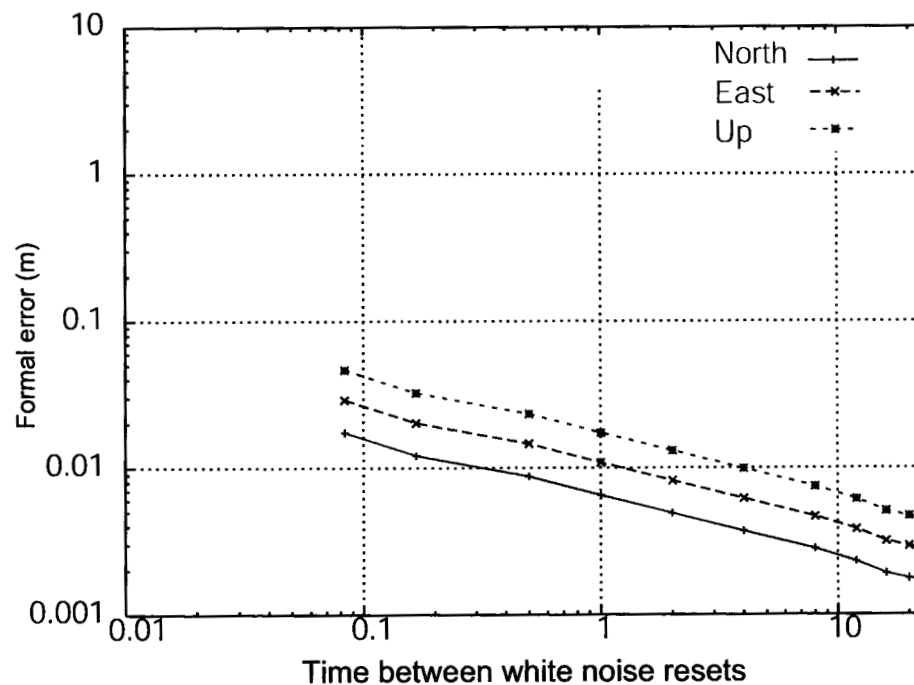
While it may seem that this is equivalent to performing whitenoise resets on the station coordinates, it is not and will significantly weaken the solution.

The top figure at right shows the formal error for for the station coordinates for rinex files of different lengths, up to 24 hours.



Compare this with the bottom figure at right. This figure shows the formal error for the station coordinates for different times between whitenoise resets, up to 24 hours.

Sub-daily solutions more frequent than every 10 hours are significantly better determined with whitenoise resets. This is in part due to the greater strength of the longer data arcs for estimating the phase bias parameters.



With data from only one station, it is impossible to pinpoint the location of preseismic slip. However, because we know the geometry and convergence direction of the plate interface, we can make a coarse estimation of the average azimuth of preseismic slip relative to AREQ. A fundamental caveat of course is that there exist an infinite number of heterogeneous slip distributions that could produce the identical offset at AREQ. The down dip location of preseismic slip cannot be constrained using the AREQ data due to the high level of noise in the vertical component. By assuming the faulting occurred along the Nazca-South American plate interface, whose location and dip are based on independent data and held fixed [Tavera and Buforn, 1998] and by fixing the preseismic focal mechanism to the rake predicted by Nuvel-1 (convergence azimuth of 75), we then allow the thrust centroid to vary along-strike and solve for the position that best replicates the observed preseismic offsets.

For the mainshock, the coseismic vector yields a best-fitting centroid that overlies the CMT location in map view. For the preseismic, the best-fitting centroid lies about 10 southeast azimuth from the aftershock CMT location implies, to the extent that one station can constrain it, the preseismic and  $M_w = 7.6$  coseismic slip are mechanistically related. This conclusion is also supported by the fact that the preseismic creep is terminated by the aftershock, which would be coincidental if the two were mechanistically unrelated.

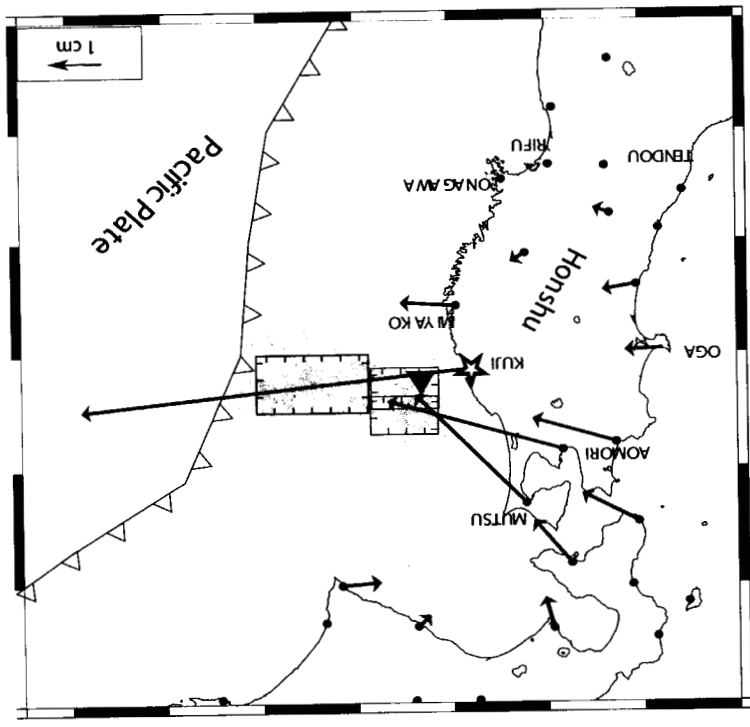
Modeling indicates that the preseismic moment is roughly a factor of two greater than the coseismic aftershock moment ( $M_w = 7.8$ ), and this is not strongly dependent on the down-dip location of the precursory slip. The presence of intermediate-rate faulting over tens of minutes is not constrained by these data but could be detected on global seismic network spectra. Teleseismically, the aftershock appears normal, and lacks any visible slow onset or rupture [Bilek and Ruff, 2002]. Thus, no inferences about creep acceleration can be made, although the GPS data do clearly illustrate a wide range of slip rates that likely reflects the interplay of variable constitutive properties.

For additional discussion on these results see

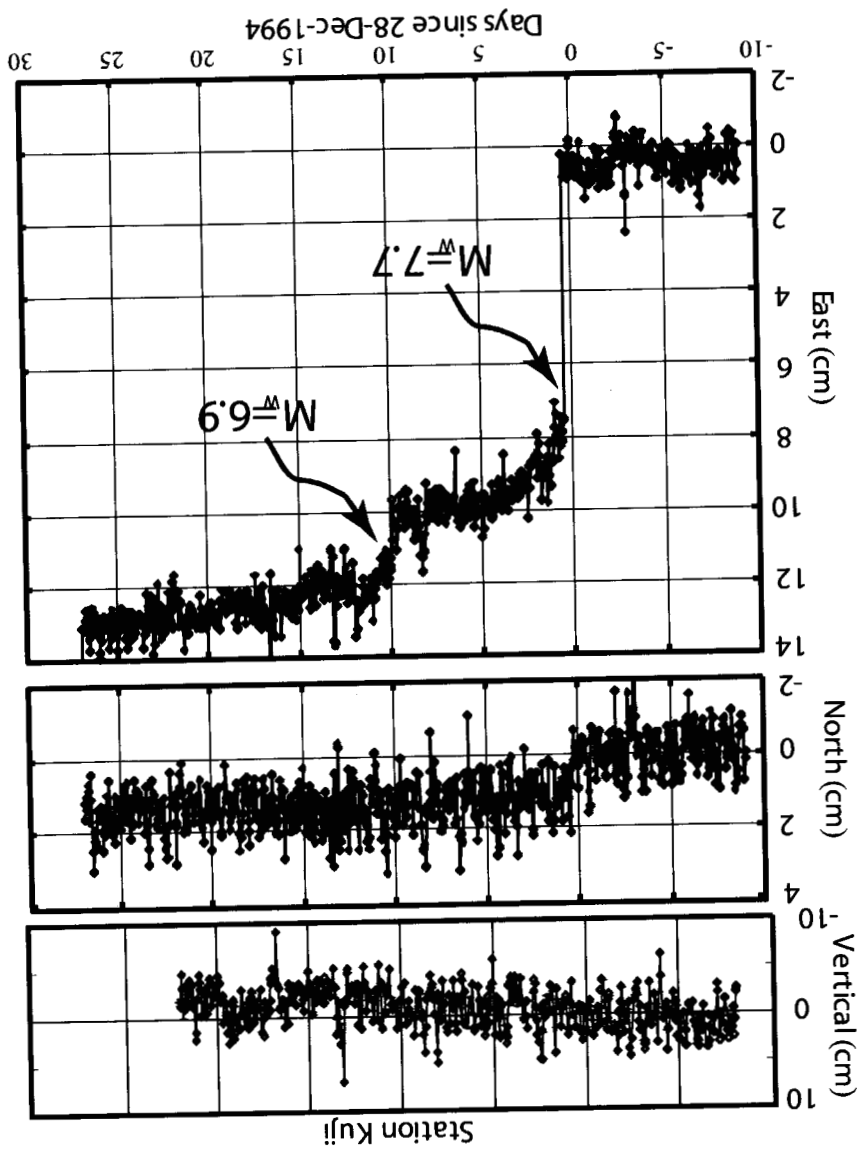
Precursory transient slip during the 2001  $M_w = 8.4$  Peru earthquake sequence from continuous GPS, T I Melbourne, F H Webb, GRL, VOL. 29, NO. 21, 2032, 2002

## Summary

Sub-daily estimates of GPS station positions is a powerful tool for detecting seismic transients when properly applied.

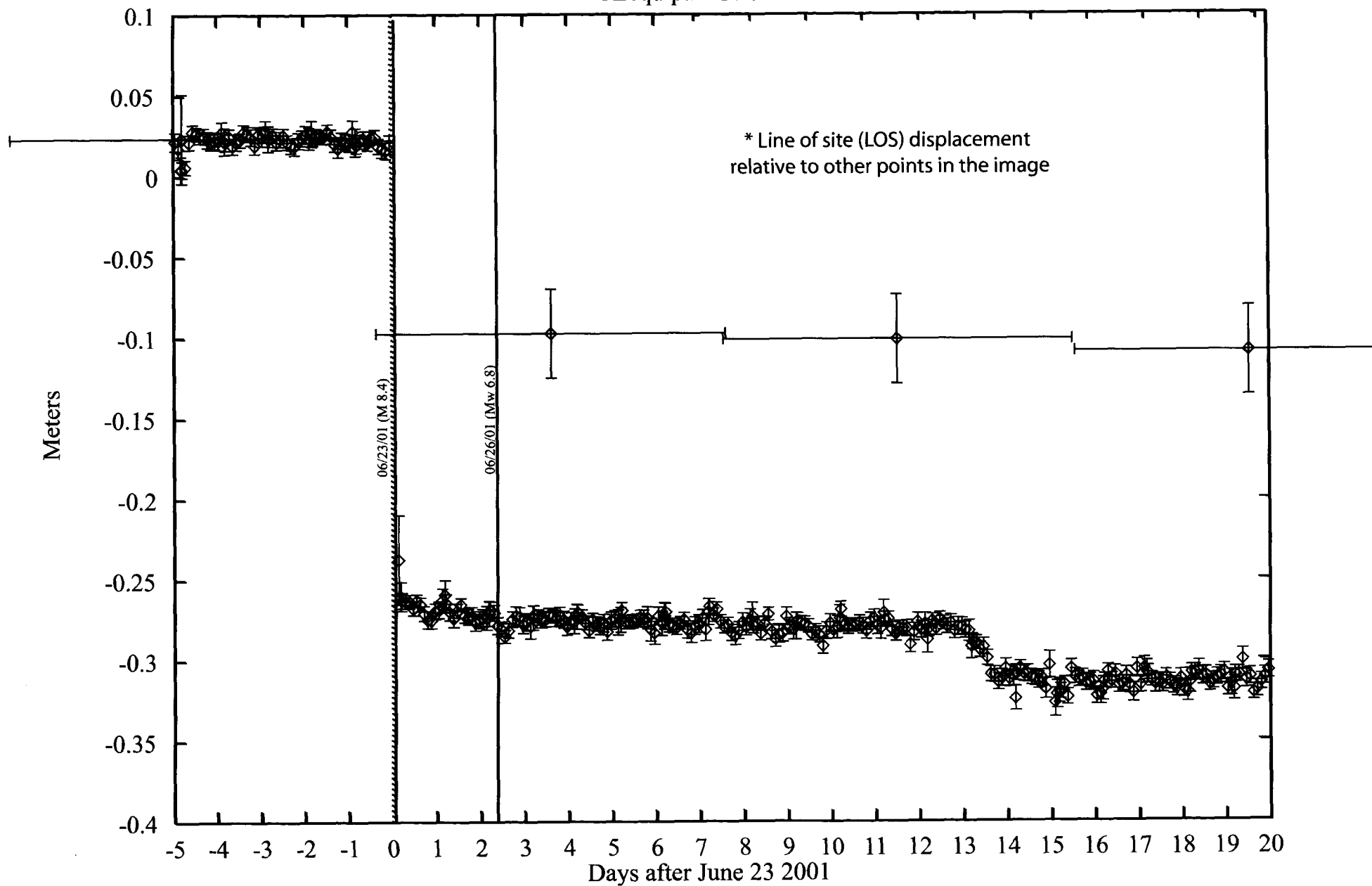


Another example of 2-hour white noise station coordinate estimates



# What would an InSAR satellite have seen?

Arequipa - LOS\*



## Synergies between InSAR and GPS

Current InSAR provides a richer data set of the spatial distribution of the deformation

(A dedicated InSAR mission could provide 3-D displacements and greater temporal resolution)

GPS can provide

Rapid displacement field

Rapid inversion

Temporal resolution

Data spanning co-seismic event

Observations of the motion of strain across the network

Continuous observations of pre-, co-, and post-seismic deformations

